JOURNAL OF GUIDANCE, CONTROL, AND DYNAMICS
Vol. 28, No. 1, January–February 2005

Spin–Yaw Lockin of an Elastic Finned Projectile

Charles H. Murphy*
Upper Falls, Maryland 21156-0269
and
William H. Mermagen Sr.†
Havre de Grace, Maryland 21078

Supersonic finned projectiles carrying very long dense metallic rods have been observed to have significantly large flexing motion. The appropriate Lagrangian for a pitching, yawing, rolling, and flexing missile is derived, and the finite element method is used to construct differential equations for finite element parameters. These differential equations for constant spin are used to calculate frequencies and damping rates of transient motion and trim response motion to missile-fixed inertia and aerodynamic forcing terms associated with inelastic deformations. The results agree with earlier results based on much more difficult iterative integration of a complex differential equation with unusual boundary conditions. Only three rod elements were necessary for reasonable accuracy. The finite element ordinary differential equations allow calculation of the time history of missile motion with varying spin and demonstrate the occurrence of spin–yaw lockin at the aerodynamic frequency and at the lowest elastic frequency.

Nomenclature

a_d = $(16L)^{-1}$
$c_{fj}(x)$ = aerodynamic force distribution functions
d = maximum rod diameter
$E(x)$ = Young's modulus
E_0 = Young's modulus at center of rod
F = complex transverse aerodynamic force, $F_y + iF_z$
$\boldsymbol{F}$ = aerodynamic force exerted on missile, nonspinning coordinates (NSC), (F_x, F_y, F_z)
g_1 = $\rho V^2 S/2$
$\mathrm{Im}\{z\}$ = imaginary part of z
I_{t0} = transverse moment of inertia of projectile about rod center
I_x = axial moment of inertia of projectile
$I(x)$ = area moment of rod,

$$(d)^4 \iint y^2 \,\mathrm{d}y\,\mathrm{d}z = (d)^4 \iint z^2 \,\mathrm{d}y\,\mathrm{d}z$$

I_0 = area moment at rod center
k = beam damping coefficient
L = rod length/rod diameter
L_e = dimensionless length of element, L/n_j
$\boldsymbol{M}$ = aerodynamic moment exerted on missile, NSC, (M_x, M_y, M_z)
m = projectile mass
n_j = number of rod elements
n_t = $2n_j + 2$
p = projectile spin
q_{bn} = finite element method (FEM) connectors, body-fixed coordinates (BFC), where $n = 3.4, \ldots, n_t$
q_n = FEM connectors, NSC, where $n = 3.4, \ldots, n_t$
q_1 = complex angle of attack of central disk, NSC, $\beta + i\alpha$
q_{le} = complex yaw and pitch of central disk, NSC, $\psi - i\theta$
q_2 = complex yaw and pitch rate of central disk, NSC, $\dot{\psi} - i\dot{\theta}$
$\mathrm{Re}\{z\}$ = real part of z
S = $\pi d^2/4$
T = total kinetic energy
T_d = kinetic energy of disk at x with thickness $\mathrm{d}x$
V = magnitude of projectile velocity
x_c = axial location of center of mass
x_{01}, x_{23} = dimensionless length of fore and aft aerodynamic extensions
x_1, x_2 = location of rod ends
α = angle of attack of central disk
β = angle of sideslip of central disk
Γ = complex cant of disk, $\partial\delta_E/\partial x$
δ_c = lateral location of missile's center of mass, NSC,

$$L^{-1}\int_{x_1}^{x_2} \delta_E \,\mathrm{d}x$$

δ_E = lateral displacement of disk, NSC, $\delta_{Ey} + i\delta_{Ez}$
ε_M = maximum strain of rod
λ_k = damping of kth mode
ρ = air density
ρ_j = axial variation of mass, moment of inertia, elasticity
σ = ω_1/ω_R
ϕ = roll angle
$\dot{\phi}_k$ = frequency of kth mode
ω_R = rigid projectile zero-spin frequency
ω_0^2 = $E_0 I_0 (L/md)$
ω_1 = lowest elastic frequency of beam in vacuum

Subscripts

B = bent projectile
BF = bent fin parameter
b = BFC parameter
E = elastic coordinate parameter, NSC
T = trim motion parameter

Presented as Paper 2003-5626 at the Atmospheric Flight Mechanics, Austin, TX, 11–13 August 2003; received 14 August 2003; revision received 20 March 2004; accepted for publication 29 March 2004.

*Consultant. Fellow AIAA.
†Consultant.

Introduction

VERY long finned projectiles carrying very dense metallic rods have been observed to be subjected to large inelastic deformations during hypersonic flight.[1] Spark shadowgraphs of these projectiles have shown elastic bending motion with amplitudes as large as the rod's radius.[2] It has been conjectured that the cause of the

inelastic deformation was the bending load associated with pitching and yawing motion at resonant spin frequencies. These frequencies would be near to the aerodynamic frequency of a rigid projectile or the elastic frequencies of the rod.

Spinning motion at a resonant frequency can be caused by a nonlinear roll moment associated with the roll orientation of the fins or by mass asymmetry due to damage or poor construction of the projectile. This spin–yaw lockin mechanism has been discussed for a rigid missile by several authors.[3–7]

The linear flight motion of an elastic missile has been considered in Refs. 8–13. In Ref. 11, a very simple theoretical model of a projectile composed of three components connected by two bent massless elastic beams was used to approximate an elastic missile. For appropriate selection of beam parameters, spin–yaw lockin was demonstrated and large-amplitude oscillations occurred. In Refs. 12 and 13, the linear partial differential equation for a continuously elastic missile was derived and special solutions for harmonic transient motion and trim motion were obtained. A nonlinear roll moment was shown to be capable of producing equilibrium spin near resonance. Although the lateral motion of the pitching and yawing missile was linearized, it was necessary to retain the quadratic terms in the roll equation. A time history of motion going to lockin was not obtained at that time. It is the purpose of this paper to compute such a time history by use of the finite element method.[14]

The lateral motion of a symmetric rigid missile has often been described by complex variables,[15] and complex variables were used in Refs. 8 and 11–13 to describe the lateral flexing motion of the rotationally symmetric rod. The equations of motion of a spinning missile are usually derived by vector analysis and Newtonian mechanics, but finite element method equations for elastic bodies require the use of the more sophisticated Lagrangian mechanics. The Lagrangian of a system must be stated in body-fixed coordinates. Separate differential equations in the two lateral directions can be obtained from the appropriate Lagrangian. Pairs of equations are combined and complex variables introduced to yield half as many complex equations.

If 5 elements are used to describe the pitching and flexing motion of the missile, 20 parameters, commonly called connectors, are introduced and 25 second-order differential equations and 1 first-order differential equation are required. The introduction of complex angles and complex connections reduce this system to 12 second-order complex differential equations and 2 real differential equations.

Coordinate System

The elastic missile is assumed to consist of a very heavy elastic circular rod of fineness ratio L and mass m embedded in a very light symmetric aerodynamic structure that may be longer than the rod. The rod's axial moment of inertia is I_x and its transverse moment of inertia about its center is I_{t0}. The rod's diameter can vary over its length, and its maximum diameter will be denoted by d. All distances will be expressed as multiples of the rod diameter, and its length is Ld. A nose windshield of length $x_{23}d$ may be attached to the forward end of the rod, and the fins may extend beyond the end of the rod a distance $x_{01}d$. Thus, the rod is located between $x_1 = -L/2$ and $x_2 = L/2$, whereas the aerodynamic structure extends from $x_0 = x_1 - x_{01}$ to $x_3 = x_2 + x_{23}$.

An Earth-fixed coordinate system will be used with the X_e axis oriented along the initial direction of the missile's velocity vector. The Z_e axis is downward pointing, and the Y_e axis is determined by the right-hand rule. A nonrotating coordinate system XYZ is then defined with the origin always at the center of the rod and the X axis tangent there. The X axis pitches through the angle θ and yaws through the angle ψ, with respect to the X_e axis. Body-fixed coordinates XY_bZ_b are now defined for which the Y_b–Z_b axes rotate with the missile though the roll angle ϕ with respect to the Y–Z axes.

We will conceptually slice the missile into a large number of thin disks perpendicular to the X axis with thickness dx. When the rod flexes, the disks shift laterally perpendicular to the X axis and cant to be perpendicular to the centerline of the disks. This canting action neglects the shear deformation of the rod, and this constraint is called

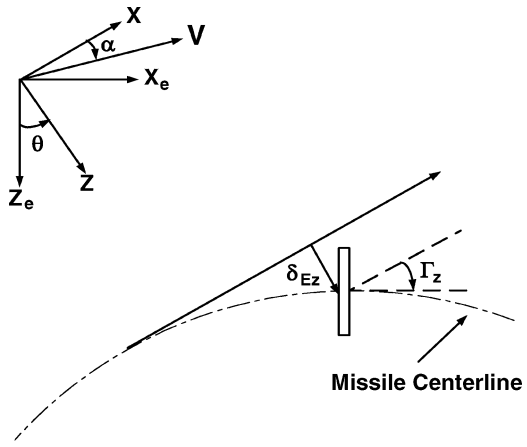

Fig. 1 ***X–Z* coordinates of cross-sectional disk.**

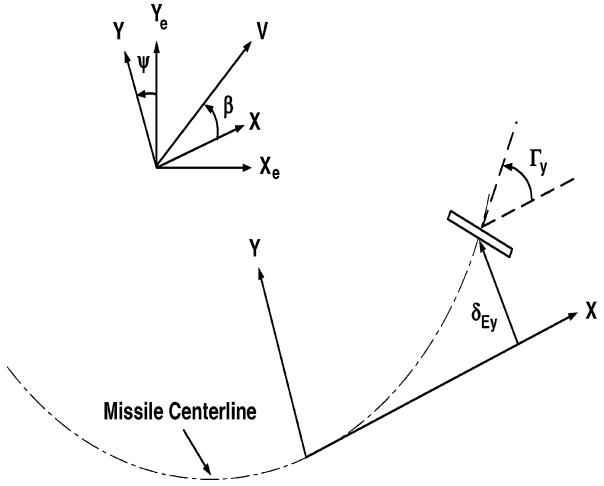

Fig. 2 ***X–Y* coordinates of cross-sectional disk.**

the Bernoulli assumption (see Ref. 14). The lateral displacement of a disk has body-fixed coordinates δ_{by} and δ_{bz}, and the disk is canted at angles Γ_{by} and Γ_{bz}:

$$\Gamma_{by} = \frac{\partial \delta_{by}}{\partial x}, \qquad \Gamma_{bz} = \frac{\partial \delta_{bz}}{\partial x} \tag{1}$$

Note that at the central disk

$$\delta_{by}(0,t) = \delta_{bz}(0,t) = \Gamma_{by}(0,t) = \Gamma_{bz}(0,t) = 0 \tag{2}$$

In Ref. 12, the nonspinning elastic coordinate system with XYZ axes ($\phi = 0$) was used. The lateral displacements of a disk in this elastic coordinate system are shown in Figs. 1 and 2 and can be computed from body-fixed quantities,

$$\delta_E = \delta_{Ey} + i\delta_{Ez} = (\delta_{by} + i\delta_{bz})e^{i\phi} \tag{3}$$

$$\Gamma = \Gamma_y + i\Gamma_z = (\Gamma_{by} + i\Gamma_{bz})e^{i\phi} \tag{4}$$

The Earth-fixed coordinates of the central disk are x_e, y_e and z_e, and the Earth-fixed coordinates of the other disks are computed in terms of the central disk Earth-fixed coordinates, their body-fixed displacements, and the Euler angles θ, ψ, and ϕ.

$$x_{de} = x_e + x\lfloor 1 - (\psi^2 + \theta^2)/2 \rfloor - \psi\,\mathrm{Re}\left\{(\delta_{by} + i\delta_{bz})e^{i\phi}\right\} + \theta\,\mathrm{Im}\left\{(\delta_{by} + i\delta_{bz})e^{i\phi}\right\} \tag{5}$$

$$y_{de} = y_e + x\psi + \mathrm{Re}\left\{(\delta_{by} + i\delta_{bz})e^{i\phi}\right\} \tag{6}$$

$$z_{de} = z_e - x\theta + \mathrm{Im}\left\{(\delta_{by} + i\delta_{bz})e^{i\phi}\right\} \tag{7}$$

The variables y_e, z_e, θ, ψ, δ_{by}, and δ_{bz} and their derivatives are assumed to be small quantities, but x_e and $\dot{x}_e$ are not small. Lagrangian dynamics yields the correct linearized differential equations for these six variables when the kinetic energy expansion retains all quadratic terms in these variables. Thus, Eqs. (6) and (7) consist of only linear terms, but Eq. (5), which contains x_e, retains quadratic terms in these variables. The coefficient of x in Eq. (5), for example, is the quadratic form of the cosine of the angle between the X_e axis and the X axis.

The angular velocity of the central disk in the body-fixed coordinates is

$$p = \dot{\phi} - \dot{\psi}\theta \tag{8}$$

$$q_b = \mathrm{Re}\{(\dot{\theta} + i\dot{\psi})e^{-i\phi}\} \tag{9}$$

$$r_b = \mathrm{Im}\{(\dot{\theta} + i\dot{\psi})e^{-i\phi}\} \tag{10}$$

The angular velocity of any other disk along axes aligned with the disk's axes of symmetry is

$$p_d = p(1 - \Gamma\bar{\Gamma}/2) + q_d\Gamma_{by} + r_d\Gamma_{bz} = p + \mathrm{Re}\{(\dot{\theta} + i\dot{\psi} - i\dot{\Gamma})\bar{\Gamma}\} \tag{11}$$

$$q_d = q_b - \dot{\Gamma}_{bz} - \dot{\phi}\Gamma_{by} = \mathrm{Re}\{(\dot{\theta} + i\dot{\psi} + i\dot{\Gamma})e^{-i\phi}\} \tag{12}$$

$$r_d = r_b + \dot{\Gamma}_{by} - \dot{\phi}\Gamma_{bz} = \mathrm{Im}\{(\dot{\theta} + i\dot{\psi} + i\dot{\Gamma})e^{-i\phi}\} \tag{13}$$

Motion of Central Disk

The mass of each circular disk is $(m/L)\rho_1(x)\,\mathrm{d}x$, its roll moment of inertia is $2a_d(md^2)\rho_2(x)\,\mathrm{d}x$, and its transverse moment of inertia is $a_d(md^2)\rho_2(x)\,\mathrm{d}x$, where a_d is $(16L)^{-1}$. Here $\rho_1(x)$ and $\rho_2(x)$ describe the variation of mass and moments of inertia along the rod, and both become unity for a homogeneous rod with constant diameter. The kinetic energy of a disk is, therefore,

$$T_d\,\mathrm{d}x = \Big\lfloor \big(md^2\rho_1/2L\big)\big(\dot{x}_{de}^2 + \dot{y}_{de}^2 + \dot{z}_{de}^2\big) + \big(a_d md^2\rho_2/2\big)\big(2p_d^2 + q_d^2 + r_d^2\big)\Big\rfloor\,\mathrm{d}x \tag{14}$$

The total kinetic energy of the missile can be obtained by integrating T_d over the length of the rod,

$$T = \int_{x_1}^{x_2} T_d\,\mathrm{d}x = T_R + md^2(T_{11} + T_{12}) + \left(\frac{md^2}{2L}\right)(T_{21} + T_{22}) \tag{15}$$

where

$$T_R = \left(\frac{md^2}{2}\right)\big(\dot{x}_e^2 + \dot{y}_e^2 + \dot{z}_e^2\big) + \frac{I_x p^2}{2} + \frac{I_{t0}(\dot{\psi}^2 + \dot{\theta}^2)}{2} + md^2 x_c[\dot{y}_e\dot{\psi} - \dot{z}_e\dot{\theta} - \dot{x}_e(\psi\dot{\psi} + \theta\dot{\theta})]$$

$$T_{11} = -\dot{x}_e\,\mathrm{Re}\{(\psi + i\theta)\dot{\delta}_c + (\dot{\psi} + i\dot{\theta})\delta_c\}$$

$$T_{12} = \mathrm{Re}\{(\dot{y}_e - i\dot{z}_e)\dot{\delta}_c + (\dot{\psi} + i\dot{\theta})(\dot{J}_6 + J_8)\}$$

$$T_{21} = \int_{x_1}^{x_2}\big(\dot{\delta}_{Ey}^2 + \dot{\delta}_{Ez}^2\big)\rho_1\,\mathrm{d}x + (a_d L)\int_{x_1}^{x_2}\big(\dot{\Gamma}_y^2 + \dot{\Gamma}_z^2\big)\rho_2\,\mathrm{d}x$$

$$T_{22} = 2\dot{\phi}(a_d L)\mathrm{Re}\left\{\int_{x_1}^{x_2}(2i\dot{\Gamma} - \dot{\phi}\Gamma)\bar{\Gamma}\rho_2\,\mathrm{d}x\right\}$$

$$x_c = \left(\frac{1}{L}\right)\int_{x_1}^{x_2} x\rho_1\,\mathrm{d}x$$

J_6 and J_8 are defined in Appendix A.

The y_e and z_e components of the central disk velocity can be approximated by linear relations in angles of pitch and yaw with respect to inertia axes θ and ψ and angles of attack and sideslip with respect to the velocity vector $\boldsymbol{\alpha}$ and $\boldsymbol{\beta}$ as shown in Figs. 1 and 2. The magnitude of the velocity vector is V,

$$\dot{y}_e = (V/d)(\boldsymbol{\beta} + \psi) \tag{16}$$

$$\dot{z}_e = (V/d)(\boldsymbol{\alpha} - \theta) \tag{17}$$

Equations (16) and (17) can be written as a single complex equation,

$$\dot{y}_e + i\dot{z}_e = (V/d)(q_1 + q_{1e}) \tag{18}$$

where

$$q_1 = \beta + i\alpha, \qquad q_{1e} = \psi - i\theta$$

In Ref. 12, the linear aerodynamic force loading is expressed in terms of three force distribution functions, $c_D(x)$, $c_{f1}(x)$, and $c_{f2}(x)$, and the base pressure coefficient C_{Dbp}, plus a body-fixed force associated with possible bent fins. Because the lateral motion of the missile is quite small, $\dot{q}_1 \cong -\dot{q}_{1e}$, and the aerodynamic damping force terms in the aerodynamic loading on the aerodynamic structure can be combined. This aerodynamic loading in nonrotating elastic coordinates is

$$\frac{\mathrm{d}F_x}{\mathrm{d}x} = -g_1 c_D(x) \tag{19}$$

$$\frac{\mathrm{d}F_y}{\mathrm{d}x} + i\frac{\mathrm{d}F_z}{\mathrm{d}x} = -g_1\left[c_{f1}(x)\left[q_1 - \Gamma - \Gamma_{\mathrm{BF}}(x)e^{i\phi} + (\dot{\delta}_E - x\dot{q}_1)\left(\frac{d}{V}\right)\right] + c_{f2}(x)\big(2\dot{q}_1 - \dot{\Gamma} - i\dot{\phi}\Gamma_{\mathrm{BF}}(x)e^{i\phi}\big)\left(\frac{d}{V}\right)\right] \tag{20}$$

$$F_{xbp} = -g_1 C_{Dpb} \tag{21}$$

The total aerodynamic force acting on the aerodynamic structure is given by the integrals of Eqs. (19) and (20) and by adding the base drag of Eq. (21) to the axial force,

$$F_x = -g_1 C_D = -g_1\left[\int_{x_0}^{x_3} c_D(x)\,\mathrm{d}x + C_{Dbp}\right] \tag{22}$$

$$F = -g_1\big\lfloor c_1 q_1 + c_2(\dot{q}_1\,d/V) - C_{N\mathrm{BF}}e^{i\phi} - J_1(t) - \dot{J}_2(t)(d/V)\big\rfloor \tag{23}$$

where various functions are defined in Appendix A.

Similarly, the transverse aerodynamic moment about the missile's center of mass for $x_c = 0$ can be computed from the transverse aerodynamic force and a small axial force contribution:

$$M = M_y + iM_z = -i(g_1 d)\big[c_3 q_1 + c_4(\dot{q}_1 d/V) - C_{M\mathrm{BF}}e^{i\phi} - J_3(t) - \dot{J}_4(t)(d/V) - J_5(t)\big] \tag{24}$$

The motion of the central disk is described by the variables x_e, y_e, z_e, ϕ, ψ, and θ, and the motion of any other section on the aerodynamic structure located at x with thickness dx is the sum of this motion plus its motion relative to the central disk. The work done on any section caused by motion of the central disk is

$$(dW_{cd})_x dx = dQ_{1x}dx_e + dQ_{1y}dy_e + dQ_{1z}dz_e + dQ_{2x}d\phi + dQ_{2y}dq_{1ey} + dQ_{2z}dq_{1ez} \tag{25}$$

where the sectional generalized forces are defined in Appendix B. The total generalized forces can be obtained by integrating the sectional generalized forces and adding the work done by the base pressure drag. These are also given in Appendix B.

The linearized Lagrangian differential equation for x_e and ϕ give the usual drag and spin equation,

$$m\dot{V} \cong m\ddot{x}_e = -g_1 C_D \tag{26}$$

$$I_x\ddot{\phi} = M_x \tag{27}$$

The Lagrangian differential equation for z_e can be multiplied by i and added to the Lagrangian differential equation for y_e to yield a single second-order differential equation in complex variables. Next the Lagrangian differential equation for θ can be multiplied by i and subtracted from the Lagrangian differential equation for ψ,

$$m\lfloor V(\dot{q}_1+q_2) + \dot{V}q_1 + \ddot{\delta}_c d + \dot{q}_2 x_c d\rfloor = F \tag{28}$$

$$I_t\dot{q}_2 - i\dot{\phi}I_x q_2 + md^2\lfloor \ddot{J}_6 + \dot{J}_8 + x_c\ddot{\delta}_c\rfloor = -iM - x_c F d \tag{29}$$

where

$$\delta_c = \left(\frac{1}{L}\right)\int_{x_1}^{x_2} \delta_E \rho_1 \,\mathrm{d}x$$

$$q_2 = \dot{q}_{1e}, \qquad I_t = I_{t0} + md^2 x_c^2$$

These differential equations for $x_c = 0$ are the same as those derived by Newtonian mechanics in Ref. 12. Equations (28) and (29) contain eight integrals of δ_E and Γ. Three of these are integrals of dynamics properties δ_c, J_6, and J_8 over the rod (x_1, x_2) and five are integrals over aerodynamic properties J_1, J_2, J_3, J_4, and J_5 over the aerodynamic structure (x_0, x_3).

For constant spin and velocity and a rigid unbent missile with its center of mass at the rod center, Eqs. (28) and (29) predict a simple epicyclic angular motion,

$$q_1 = K_{10}\exp(\lambda_1 t + i\phi_1) + K_{20}\exp(\lambda_2 t + i\phi_2) \tag{30}$$

where

$$\dot{\phi}_m = \dot{\phi}I_x/2I_t \pm \sqrt{-(g_1 d/I_t)c_3 + (\dot{\phi}I_x/2I_t)^2}$$

For zero spin, $\dot{\phi}_1 = -\dot{\phi}_2 = \omega_R$, where $\omega_R = \sqrt{[(g_1 d/I_t)|c_3|]}$.

Finite Element Method

The rod is assumed to be represented by the sum of an inelastic bent component rotating with the missile and an elastic deformation,

$$\delta_E(x,t) = \delta_{EB}(x)e^{i\phi} + \tilde{\delta}_E(x,t), \qquad x_1 \le x \le x_2 \tag{31}$$

$$\delta_b(x,t) = \delta_{EB}(x) + \tilde{\delta}_b(x,t), \qquad x_1 \le x \le x_2 \tag{32}$$

where

$$\delta_{EB}(0) = \frac{\mathrm{d}\delta_{EB}(0)}{\mathrm{d}x} = 0$$

Because the aerodynamic structure is rigidly attached to the rod,

$$\delta_E(x,t) = \delta_E(x_1,t) + (x-x_1)\Gamma(x_1,t), \qquad x_0 \le x \le x_1 \tag{33}$$

$$\delta_E(x,t) = \delta_E(x_2,t) + (x-x_2)\Gamma(x_2,t), \qquad x_2 \le x \le x_3 \tag{34}$$

The motion of the elastic component of the rod is controlled by the elasticity of the rod and the aerodynamic force acting on it.

The finite element method (FEM) is a powerful method for calculating the time history of elastic flexing motion. The rod is divided into n_j elements of non-dimensional length $L_e = L/n_j$. The shape of the jth element is given by a linear combination of third-order Hermitian polynomials (Appendix B),

$$\tilde{\delta}_{by}(x,t) = \sum_1^4 \hat{q}_{bpy}(t)N_p(z) \tag{35}$$

$$\tilde{\delta}_{bz}(x,t) = \sum_1^4 \hat{q}_{bpz}(t)N_p(z) \tag{36}$$

where

$$x = L_e(z + z_j), \qquad z_j = x_1/L_e + j - 1, \qquad 0 \le z \le 1$$

The coefficients of the polynomials are functions of time and are called connectors. The first two are the deflection and slope of the left end of the element, and the third and fourth are the deflection and slope of the right end. To assure continuity in deflection and slope at junction points, the corresponding pairs of connectors are equal. We will consider only an odd number of elements and require that the connecters of the central element satisfy Eq. (2). Thus,

$$\hat{q}_{b3} = 5\hat{q}_{b1} + L_e\hat{q}_{b2} \tag{37}$$

$$\hat{q}_{b4} = 24L_e^{-1}\hat{q}_{b1} + 5\hat{q}_{b2} \tag{38}$$

where

$$\hat{q}_{bq} = \hat{q}_{bqy} + \hat{q}_{bqz}$$

For n_j elements, there are $2n_j$ independent complex connectors. It is convenient to let the index for the connectors run from 3 to n_t, where $n_t = 2n_j + 2$.

The usual FEM procedure calculates the elastic parts of the integrals in Eqs. (28) and (29) by first obtaining integrals over each element. These are linear functions of that element's four connector functions. Because of Eqs. (37) and (38), the central element has only two independent connector functions and the next adjacent element connector functions are related to them. Integrals for these elements are specially computed. The desired elastic integrals are sums of these subintegrals and are linear combinations of the $2n_j$ complex connector functions. The three dynamic integrals can be written as

$$\delta_c = L^{-1}\sum_3^{n_t} a_{1n}q_n + \delta_{cB}e^{i\phi} \tag{39}$$

$$J_6 = L^{-1}\sum_3^{n_t} a_{2m}q_n + J_{6B}e^{i\phi} \tag{40}$$

$$J_8 = a_d\sum_3^{n_t} b_{2n}(\dot{q}_n - 2i\dot{\phi}q_n) + i\dot{\phi}J_{8B1}e^{i\phi} \tag{41}$$

where

$$q_n = q_{bn}e^{i\phi}$$

The five aerodynamic integrals have contributions from the aerodynamic structure extensions as well as from each element,

$$J_1 + \dot{J}_2\left(\frac{d}{V}\right) = \sum_3^{n_t}\left[(f_{1n} + f_{a1n})q_n + (g_{1n} + g_{a1n})\left(\frac{\dot{q}_n d}{V}\right)\right] + \left[J_{1B} + i\left(\frac{\dot{\phi}d}{V}\right)J_{2B}\right]e^{i\phi} \tag{42}$$

$$J_3 + \dot{J}_4\left(\frac{d}{V}\right) = \sum_3^{n_t}\left[(f_{2n} + f_{a2n})q_n + (g_{2n} + g_{a2n})\left(\frac{\dot{q}_n d}{V}\right)\right] + \left[J_{3B} + i\left(\frac{\dot{\phi}d}{V}\right)J_{4B}\right]e^{i\phi} \tag{43}$$

$$J_5 = \sum_3^{n_t}\left(-C_D a_{1n}L^{-1} + h_{an}\right)q_n + J_{5B}e^{i\phi} \tag{44}$$

Expressions for computing δ_{cB}, J_{kB}, and h_{an} and all FEM coefficients in Eqs. (39–44) for one, three, five, and seven elements are given in Ref. 16.

Equations (39–44) can be used with Eqs. (28) and (29) to write these two complex differential equations in a standard format:

$$\sum_{n=1}^{n_t}\left[R_{mn}\ddot{q}_n + \left(S_{mn} + i\dot{\phi}S^*_{mn}\right)\dot{q}_n + \left(T_{mn} + i\dot{\phi}T^*_{mn}\right)q_n\right] = t_m \exp(i\phi) \tag{45}$$

where

$$t_m = (md^2)t_{mD} + (g_1 d)t_{mA}$$

The coefficients for $m = 1, 2$ are given in Appendix C.

Flexing Motion

To derive the equations for flexing motion, the kinetic energy given by Eq. (15) must be expressed in terms of rigid-body parameters plus the connector functions. The usual FEM process can be used to express the T_{2j} in terms of two matrices, two vectors, and two constants,

$$T_{21} = \sum_{3}^{n_t}\sum_{3}^{n_t} k_{mn}[\dot{q}_{my}\dot{q}_{ny} + \dot{q}_{mz}\dot{q}_{zn}] - 2\mathrm{Re}\left\{i\dot{\phi}e^{-i\phi}\sum_{3}^{n_t} k_{Bm}\dot{q}_m\right\} + \dot{\phi}^2 I_{xB1}L \tag{46}$$

$$T_{22} = 2\dot{\phi}a_d L\mathrm{Re}\left\{i\sum_{3}^{n_t}\sum_{3}^{n_t} b_{mn}(2i\dot{q}_m - \dot{\phi}q_m)\bar{q}_n + 2ie^{-i\phi}\sum_{3}^{n_t}\bar{b}_{Bn}(\dot{q}_m + 2i\dot{\phi}q_m)\right\} + \dot{\phi}^2 I_{xB2}L \tag{47}$$

Computation formulas for k_{mn}, k_{Bn}, b_{mn}, b_{Bn}, I_{xB1}, and I_{xB2} are given in Ref. 16.

The potential energy (PE) stored by elastic deformation is

$$\mathrm{PE} = \left(\frac{1}{2}\right)\int_{x_1}^{x_2}\left(\frac{EI}{d}\right)\left[\left(\frac{\partial^2\tilde{\delta}_{by}}{\partial x^2}\right)^2 + \left(\frac{\partial^2\tilde{\delta}_{bz}}{\partial x^2}\right)^2\right]\mathrm{d}x \tag{48}$$

where

$$E(x)I(x) = E_0 I_0 \rho_3(x)$$

E_0 and I_0 are values of Young's modulus and the area moment of inertia at the rod's center, and $\rho_3(x)$ gives the variation of their product along the rod. For a homogeneous rod with constant diameter, the product is unity. The potential energy integral can be replaced by a sum of integrals over each of the n_j elements. After integration over each element, the results can be summed to yield a linear combination of the $4n_j$ real connectors,

$$V = \left(\frac{md^2\omega_0^2}{2L}\right)\sum_{m=3}^{n_t}\sum_{n=3}^{n_t}(q_{bmy}q_{bny} + q_{bmz}q_{bnz})c_{mn} \tag{49}$$

where

$$\omega_0^2 = E_0 I_0 L/md^3$$

Formulas for computing c_{mn} are given in Ref. 16.

The work done on the rod by this elastic force can be expressed in terms of generalized force terms,

$$\mathrm{d}W_E = \left(\frac{md^2}{L}\right)\omega_0^2\sum_{m=3}^{n_t}[Q_{Emy}\,\mathrm{d}q_{bmy} + Q_{Emz}\,\mathrm{d}q_{bmz}] \tag{50}$$

where

$$Q_{Emy} + iQ_{Emz} = -\sum_{n=3}^{n_t} c_{mn}q_{bn}$$

The Kelvin–Voight elastic damping force (see Ref. 17) that is proportional to the time derivative of the elastic shear force has generalized force terms:

$$\mathrm{d}W_D = \left(\frac{md^2}{L}\right)\omega_0^2\sum_{m=3}^{n_t}[Q_{Dmy}\,\mathrm{d}q_{bmy} + Q_{Dmz}\,\mathrm{d}q_{bmz}] \tag{51}$$

where

$$Q_{Dmy} + iQ_{Dmz} = -\left[\frac{2\hat{k}}{\omega_1}\right)\sum_{n=3}^{n_t} c_{mn}\dot{q}_{bn}$$

$$\omega_1 = (4.730/L)^2\omega_0$$

The scale factor $2\omega_1^{-1}$ is selected so that $\hat{k} = 1$ corresponds to critical damping of the first elastic mode.

The external aerodynamic force is divided between the force acting on the rod and the force acting on the aerodynamic structure extensions at the ends of the rod. The total work done on the missile is the sum of the work done by these forces,

$$\mathrm{dW}_A = \sum_{j=1}^{n_j}[\mathrm{d}W_{Aj} + \mathrm{d}W_{a1} + \mathrm{d}W_{an_j}] = (g_1\,\mathrm{d})\sum_{m=3}^{n_t}[Q_{Amy}\,\mathrm{d}q_{bmy} + Q_{Amz}\,\mathrm{d}q_{bmz}] \tag{52}$$

where

$$Q_{Amy} + iQ_{Amz} = \sum_{n=3}^{n_t}\left[(f_{mn} + f_{amn})q_n + (g_{mn} + g_{amn})\left(\frac{\dot{q}_n d}{V}\right)\right]e^{-i\phi} + f_{Bm} + f_{aBm} + i\left(\frac{\dot{\phi}d}{V}\right)(g_{Bm} + g_{aBm})$$

Formulas for computing f_{mn}, g_{mn}, f_{amn}, g_{amn}, f_{Bm}, g_{Bm}, f_{aBm}, and g_{aBm} are given in Ref. 16.

Equations (50–52) in conjunction with the kinetic energy defined by Eqs. (15), (46), and (47) can be used to derive the $4n_j$ Lagrangian differential equations for the q_{bmy} and q_{bmz} for $m = 3, 4, \ldots, 2n_j + 2$. The equation for q_{bmz} should be multiplied by i and added to the corresponding equation for q_{bmy} to yield $2n_j$ complex differential equations for the complex variables q_{bm}. If the q_{bm} are replaced by q_m in each equation, the result has the standard form given by Eq. (45) where the $14n_j$ complex coefficients for $m = 3, 4, \ldots, 2n_j + 2$ are given in Appendix C.

Special Solutions

A rigid symmetric finned missile flying with constant spin and velocity has two natural frequencies, $\dot{\phi}_{1R}$ and $\dot{\phi}_{2R}$, where $\dot{\phi}_{1R} \cong -\dot{\phi}_{2R}$. For zero spin, each of the flexure frequencies gives rise to two coning frequencies, $\pm\omega_K$. The frequencies present in the motion of an elastic projectile form an infinite sequence where the first two are related to $\dot{\phi}_{1R}$ and $\dot{\phi}_{2R}$, whereas the later ones evolve from $\pm\omega_K$, that is, $\dot{\phi}_{2K+1} \cong \omega_K$ and $\dot{\phi}_{2K+2} \cong -\omega_K$. The odd-numbered modes have positive frequencies and are called positive modes, whereas the even-numbered modes are called negative modes. For nonzero spin, the pairs of frequencies are no longer equal in magnitude.

Transient harmonic solutions of the homogeneous constant spin and velocity version of Eq. (45) have the form

$$q_m = q_{mk}e^{iAt}, \qquad A = A_k, \qquad k = 0, 1, 2, 3, \ldots, 2(2n_j + 1) \tag{53}$$

After substitution of Eq. (53) into Eq. (45), a set of linear homogeneous algebraic equations is derived that is specified by an n_t by n_t matrix,

$$u_{mn} = A^2 R_{mn} + A\left(S_{mn} + i\dot{\phi}S^*_{mn}\right) + T_{mn} + i\dot{\phi}T^*_{mn} \tag{54}$$

The damping rates and frequencies of the transient motion are given by roots of $\det(u_{mn}) = 0$.

For n_j elements there are $2n_j + 1$ pairs of positive and negative frequencies. The lowest frequency pair is related to the two aerodynamic frequencies, and the other $2n_j$ pairs are approximations of first $2n_j$ elastic frequencies of the infinite set of frequencies for the elastic rod. The paired frequencies are equal in magnitude when spin is zero, but the positive frequency has a larger magnitude when spin is positive. For an elastic beam considered by Geradin and Rixen,[14] the first n_j approximations are close to the correct values. This accuracy is determined by the ability of n_j elements to describe the corresponding mode shape correctly. Geradin and Rixen[14] also observe that the approximations are upper bounds of correct value.

For constant spin and velocity, the trim motion in response to the spinning bent missile forces can be obtained by assuming a solution of the form

$$q_n = q_{nT} e^{i\dot{\phi}t} \tag{55}$$

The response parameters q_{nT} vary with particular values of the constant spin and are solutions of a set of n_t linear inhomogeneous algebraic equations,

$$\sum_{n=1}^{n_t} B_{mn} q_{nT} = t_m \tag{56}$$

where

$$B_{mn} = -\dot{\phi}^2\left(R_{mn} + S^*_{mn}\right) + i\dot{\phi}\left(S_{mn} + T^*_{mn}\right) + T_{mn}$$

In Ref. 12, both of these special solutions were computed from iterative solutions of second-order differential equation specified by special boundary conditions. The FEM approach obtains the same results and more by much simpler matrix operations.

Quadratic Roll Equation

The linear roll equation (26) was derived from a kinetic energy function that neglected cubic terms in q_{1y}, q_{1z}, q_{2z}, q_{bny}, and q_{bnz}. To derive the quadratic roll equation, cubic terms involving ϕ and $\dot{\phi}$ must be retained. The resulting roll equation is the same as that derived in Ref. 12 from Newtonian mechanics,

$$I_x\ddot{\phi} + md^2\,\mathrm{Re}\left\{\dot{J}_7 - i\dot{q}_2\bar{J}_6 + iq_2\bar{J}_8 - iF\bar{\delta}_c\right\} = M_x \tag{57}$$

where $\dot{J}_7(t)$ is defined in Appendix A.

The aerodynamic roll moment is the X component of the aerodynamic moment about the center of the central disk. The linear roll moment coefficient for a rigid finned projectile is usually expressed in terms of a roll damping coefficient and a steady-state spin,

$$(C_\ell)_{\text{linear}} = C_{\ell p}(\dot{\phi} - p_{ss})(d/V) \tag{58}$$

The steady-state spin is usually determined by a differential canting of the fins caused either intentionally by the designer or unintentionally by damage to the projectile.

The roll moment of one of the projectile's thin disks is the sum of the linear roll moment. It has as part of a projectile and the quadratic roll moment induced by the transverse aerodynamic force acting on its lateral displacement relative to the center of the central disk. If we retain only the dominant c_{fl} term in Eq. (20), the quadratic roll moment has the form

$$\begin{aligned}(dM_x)_{\text{quadratic}} &= \lfloor (dF_z)\delta_{Ey} - (dF_y)\delta_{Ez}\rfloor \\ &= (g_1 d)c_{f1}\,\mathrm{Re}\Big\{i\Big[\left(q_1 - \Gamma - \Gamma_{\text{BF}}e^{i\phi}\right) \\ &\quad + (\dot{\delta}_E - x\dot{q}_1)(d/V)\Big]\bar{\delta}_E\Big\}\,\mathrm{d}x\end{aligned} \tag{59}$$

The total aerodynamic roll moment acting on the projectile, therefore, is

$$M_x = (g_1 d)[(C_\ell)_{\text{linear}} + \mathrm{Re}\{Q_A(t) - iF\bar{\delta}_c\}] \tag{60}$$

where

$$Q_A(t) = i\int_{x_0}^{x_3} c_{f1}\left[(\xi - \Gamma) + (\dot{\delta}_E - x\dot{q}_1)\left(\frac{d}{V}\right)\right](\bar{\delta}_E - \bar{\delta}_c)\,\mathrm{d}x$$

The nonlinear roll moment from Eq. (60) can be placed in the spin equation (57) with $\dot{J}_7$ expressed in terms of the FEM connectors to yield

$$I_X\ddot{\phi} + \mathrm{Re}\left\{md^2(Q_D - i\dot{q}_2\bar{J}_6 + iq_2\bar{J}_8) - g_1 d\,Q_A\right\} = g_1 d(C_\ell)_{\text{linear}} \tag{61}$$

Formulas for calculating the quadratic terms I_x and Q_D are given in Ref. 16.

For trim motion, $\ddot{\phi} = \mathrm{Re}\{Q_D\} = 0$ and $\dot{q}_2 = i\dot{\phi}q_{2T}e^{i\dot{\phi}t}$ and Eq. (61) becomes a simple equality of two functions of p,

$$f_2(\dot{\phi}) = f_1(\dot{\phi}) \tag{62}$$

where

$$f_1 = \dot{\phi} - p_{ss}$$

$$f_2 = -R\{Q_{AT} - (q_{2T}md/g_1)(\dot{\phi}\bar{J}_{6T} + i\bar{J}_{8T})\}(C_{\ell p}d/V)^{-1}$$

$$Q_{AT} = i\int_{x_0}^{x_3} c_{f1}\left[(q_{1T} - \Gamma_T - \Gamma_{\text{BF}}) + i(\delta_{ET} - xq_{1T})\left(\frac{\dot{\phi}d}{V}\right)\right]\bar{\delta}_T\,\mathrm{d}x$$

and where δ_{ET} and Γ_T are computed from the solution to Eq. (56) and J_{6T} and J_{8T} are J_6 and J_8 evaluated for δ_{ET} and Γ_T. For moderate spin, Q_{AT} is the dominant part of f_2. Equilibrium values of spin are determined by the intersection of these two curves. Lockin occurs at stable equilibrium spin.

Spin lockin can only occur when the missile has some rigid asymmetry such as that described by δ_{EB} or Γ_{BF}. For a rigid missile, δ_{ET} and Γ_T are δ_{EB} and Γ_B. Here q_{1T} is a function of spin, which has a large resonant amplitude when spin is near ω_R. For an elastic missile, q_{1T}, δ_{ET}, and Γ_T are all functions of spin and have large resonant amplitudes when spin is near $\dot{\phi}_{2k-1}$ for positive spin or near $\dot{\phi}_{2k}$ for negative spin.

Numerical Results

In Ref. 12, calculations were made for a 20-caliber fin-stabilized rod flying at 6000 ft/s. The finned missile has a 1-caliber nose extension and a 1-caliber fin extension (Fig. 3). The mass and aerodynamic parameters for the finned missile are given in Appendix D. A pair of quartic curves will describe the bent rod,

$$\delta_{EB}\begin{cases} = d_{11}x^2 + d_{21}x^4, & -10 \le x \le 0 \\ = d_{12}x^2 + d_{22}x^4, & 0 \le x \le 10 \end{cases} \tag{63}$$

The values of d_{ij} are given in Appendix D.

A measure of the flight flexibility of a missile is the ratio of the first elastic frequency to the rigid missile aerodynamic frequency, $\sigma \equiv \omega_1/\omega_R$. Calculations of $\dot{\phi}_1$ vs σ have been made for the one-, three-, five-, and seven-element rod. The results for all but the one-element rod are practically identical. At $\sigma = 5$, the aerodynamic frequency is 60% of the rigid-missile aerodynamic frequency, and even at $\sigma = 10$, it 10% less than the rigid-missile aerodynamic frequency.

The first six positive frequencies and their damping rates for $\sigma = 5$ have been calculated for 1, 3, 5, and 7 elements. These results together with calculations from the theory of Ref. 12 are tabulated in Table 1. We identify frequencies that differ from the Ref. 12 value by more than 10% as poor values and they are marked by an $\times$. Thus, the one-element rod yields one moderately good result, whereas the three-element and five-element rods yield three and five good results, respectively. For this elastic problem, $n_j - 1$ elastic frequencies are well calculated. For zero spin, the negative frequencies are the negatives of the positive frequencies.

Because the three-element rod predicts the lower three frequencies quite well, all of the calculations given in this paper are based

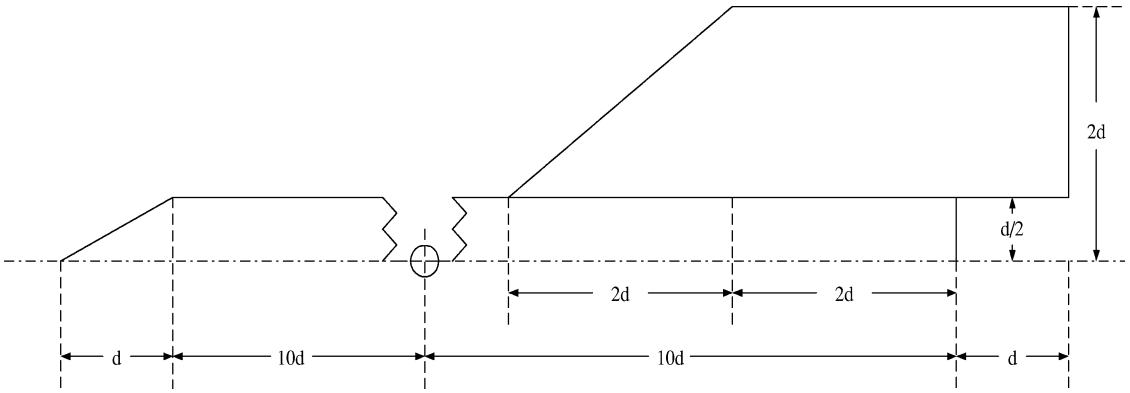

Fig. 3 Finned missile.

Table 1 Transient frequencies and damping rates[a]

Code	k	$\dot{\phi}_k/\omega_R$	λ_k/ω_R
1-elem	1	0.645	−0.0530
3-elem	1	0.612	−0.0528
5-elem	1	0.613	−0.0528
7-elem	1	0.613	−0.0528
Ref. 12	1	0.614	−0.0529
1-elem	3	6.146×	−0.0855
3-elem	3	5.194	−0.0724
5-elem	3	5.181	−0.0718
7-elem	3	5.180	−0.0717
Ref. 12	3	5.184	−0.0717
1-elem	5	20.31×	−0.0644
3-elem	5	13.81	−0.0518
5-elem	5	13.79	−0.0523
7-elem	5	13.76	−0.0518
Ref. 12	5	13.74	−0.0506
1-elem	7	×	——
3-elem	7	30.00×	−0.1018
5-elem	7	26.97	−0.0914
7-elem	7	26.79	−0.0881
Ref. 12	7	26.69	−0.0825
1-elem	9	×	——
3-elem	9	53.37×	−0.2060
5-elem	9	44.28	−0.1389
7-elem	9	44.18	−0.1462
Ref. 12	9	43.84	−0.1427
1-elem	11	×	——
3-elem	11	100.44×	−0.4708
5-elem	11	72.19×	−0.1309
7-elem	11	65.88	−0.1256
Ref. 12	11	64.49	−0.1202

[a]Here $\sigma = 5$ and $\dot{\phi} = 0$.

on a three-element rod. Most of these have been repeated for a five-element rod, and almost identical results have been obtained.

According to Table 1, the first elastic frequency for $\sigma = 5$ is near $5.2\omega_R$, and in Ref. 13, it is predicted that resonant lockin is possible for $p_{ss} = 6.5\omega_R$. Equations (45) were integrated using an explicit Runge–Kutta formula based on the Dorman–Prince scheme.[18] All initial conditions were set equal to zero except $\dot{\phi}_0 = 0, 5.4\omega_R$. For zero initial spin, resonant lockin occurs and large strains result. For the larger value of initial spin, lockin occurs near p_{ss}. This behavior was predicted by the simple three-body theory of Ref. 11.

It is very unlikely that sufficient fin damage occurs to produce a p_{ss} in excess of five times ω_R. Because it is much more likely that a p_{ss} near ω_R can be produced, the observed inelastic deformation is probably caused by lockin at the aerodynamic frequency, and this case is considered in detail next.

In Fig. 4, f_2 is plotted vs $\dot{\phi}/\omega_R$ for $\sigma = 5$ and $\Gamma_{\mathrm{BF}} = 0$. Large resonance values occur for $\dot{\phi}/\omega_R \cong 0.6$, and an f_1 line for $p_{ss} = 0.8\omega_R$ is also shown. The f_1 line has three intersections with the f_2 curve, which are values of equilibrium spin (0.590, 0.647, and 0.788). The

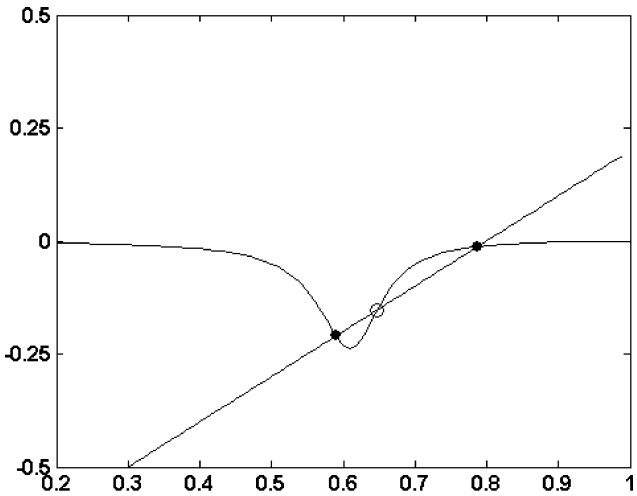

Fig. 4 Parameter f_2 vs $\dot{\phi}/\omega_R$ for $\Gamma_{\mathrm{BF}} = 0$, $\sigma = 5$, and $p_{ss} = 0.8\omega_R$.

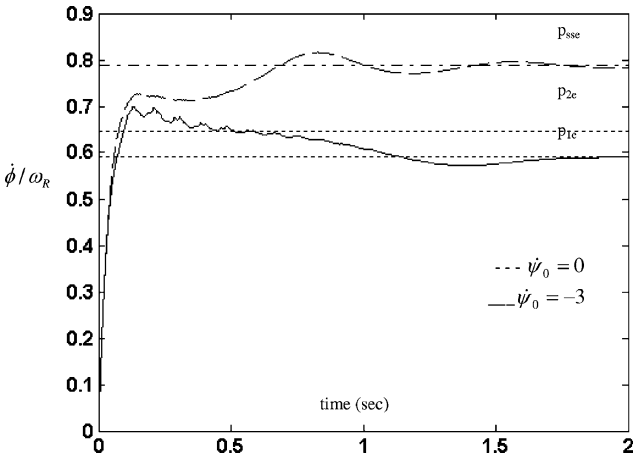

Fig. 5 Parameter $\dot{\phi}/\omega_R$ vs time for $\Gamma_{\mathrm{BF}} = 0$, $\sigma = 5$, and $p_{ss} = 0.8\omega_R$; (initial conditions all zero except $\dot{\psi}_0 = 0$ and $-3\ \mathrm{s}^{-1}$.

intersection near p_{ss}/ω_R is denoted as p_{sse}/ω_R, whereas the other two are p_{1e}/ω_R and p_{2e}/ω_R.

In Fig. 5 spin histories are plotted for $p_{ss} = 0.8\omega_R$ with zero initial conditions except for $\dot{\psi}_0 = 0$ and $-3\ \mathrm{s}^{-1}$. Here we see that p_{see} spin–yaw lockin occurs for zero initial angular velocity and p_{1e} spin–yaw lockin for an initial yaw rate of $-3\ \mathrm{s}^{-1}$. For lockin at p_{see}, the motion is smaller than 0.09 rad, whereas for lockin at p_{1e}, it is as large as 0.15 rad. The motion of the forward end of the rod in body-fixed coordinates is given in Fig. 6. Motion for p_{see} lockin is less than 0.17 (0.7 in.) and after 1 s, it is never greater than 0.09 (0.4 in.). For p_{1e} lockin, it exceeds 0.28 (1.2 in.).

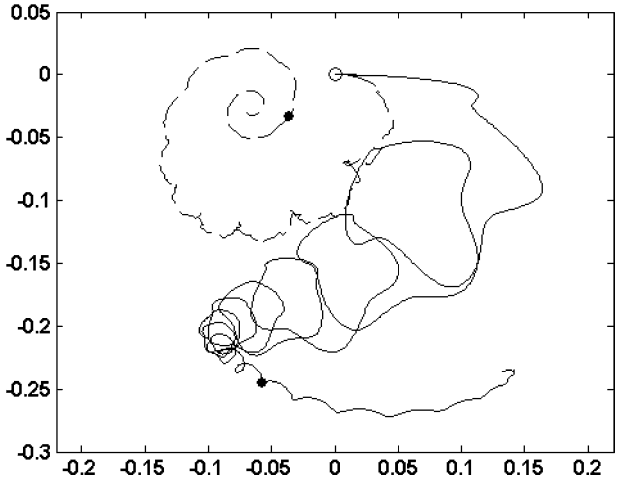

Fig. 6 Rod forward tip motion (q_{b7y} vs q_{b7z}) for $\Gamma_{BF} = 0$, $\sigma = 5$, $p_{ss} = 0.8\omega_R$, and $\dot{\psi}_0 = 0$ and -3 s^{-1}.

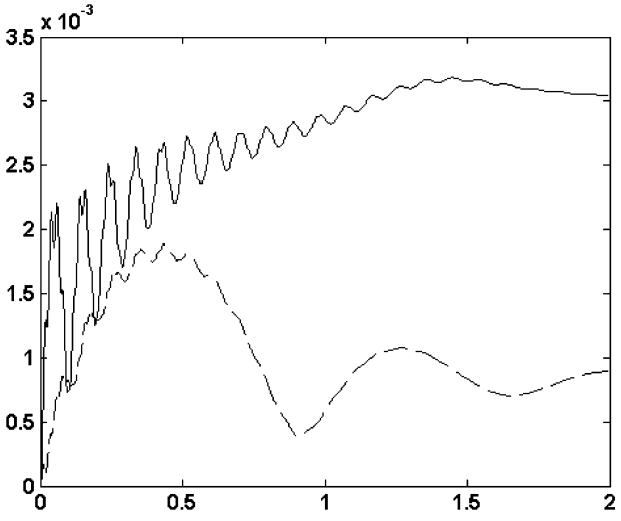

Fig. 7 Maximum strain ε_M vs time for $\Gamma_{BF} = 0$, $\sigma = 5$, $p_{ss} = 0.8\omega_R$, and $\dot{\psi}_0 = 0$ and -3 s^{-1}.

The maximum strain on the rod is located on the rod's surface at its center. Strain at this location is written in terms of three element connectors as

$$\varepsilon_M = \left(\frac{1}{2}\right)\left|\frac{\partial^2 \delta_E(0)}{\partial x^2}\right| = L_e^{-2}|12q_5 + 2L_e q_6| \tag{64}$$

The time history of the maximum strain is plotted in Fig. 7 for $\dot{\psi}_0 = 0$ and -3 s^{-1}. For most metals, yield will occur for maximum strains in excess of 0.0015, and we see that yield does occur for resonance lockin.

The two regions of the initial angular rate plane, that is, the $\dot{\psi}_0$–$\dot{\theta}_0$ plane, which induces either variety of lockin, can be determined by a number of trial and error calculations, and the boundary curve between these regions is shown in Fig. 8. Initial conditions outside this curve will cause resonance lockin, whereas conditions inside it induce p_{see} lockin.

Summary

The application of the FEM to the calculation of the motion of a pitching, yawing, and flexing missile has resulted in the construction of a family of linear differential equations.

Computer codes have been developed for one, three, five, and seven elements and used to obtain the first four elastic frequencies. The three-element code has given excellent values of the first two elastic frequencies. The five-element and seven-element codes provide equally good values of the first four elastic frequencies.

Integration of these differential equations has demonstrated resonant spin lockin at the aerodynamic frequency and the first elastic frequency. Lockin can occur near the design steady-state spin, or near resonance with a transient frequency. Calculations have identified regions of a yaw rate–pitch rate plane that determine which lockin will occur.

Appendix A: Integrals

The aerodynamic coefficients are

$$c_1 = C_{N\alpha} = \int_{x_0}^{x_3} c_{f1}\,\mathrm{d}x$$

$$c_2 = C_{Nq} + C_{N\dot{\alpha}} = \int_{x_0}^{x_3} c_{f3}\,\mathrm{d}x, \qquad c_3 = C_{M\alpha} = \int_{x_0}^{x_3} c_{f1}x\,\mathrm{d}x$$

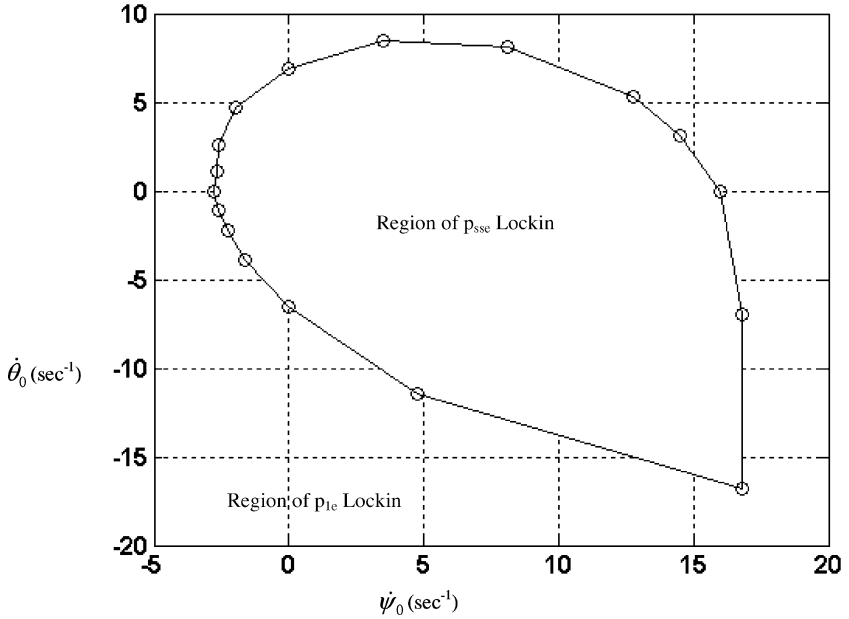

Fig. 8 Parameter $\dot{\psi}_0$ vs $\dot{\theta}_0$ showing regions of p_{sse}, p_{le} lockin, $\Gamma_{BF} = 0$, $\sigma = 5$, and $p_{ss} = 0.8\omega_R$.

$$c_4 = C_{Mq} + C_{M\dot{\alpha}} = \int_{x_0}^{x_3} c_{f3} x \, \mathrm{d}x$$

$$C_{N\mathrm{BF}} = \int_{x_0}^{x_3} c_{\mathrm{BF}} \Gamma_{\mathrm{BF}} \, \mathrm{d}x, \qquad C_{M\mathrm{BF}} = \int_{x_0}^{x_3} c_{\mathrm{BF}} \Gamma_{\mathrm{BF}} x \, \mathrm{d}x$$

$$c_{f3} = 2c_{f2} - xc_{f1}, \qquad c_{\mathrm{BF}} = c_{f1} + (\dot{\phi} d/V) c_{f2}$$

The functions of time are

$$\delta_c(t) = \left(\frac{1}{L}\right) \int_{x_1}^{x_2} \delta_E \rho_1 \, \mathrm{d}x, \qquad J_1(t) = \int_{x_0}^{x_3} c_{f1} \Gamma \, \mathrm{d}x$$

$$J_2(t) = \int_{x_0}^{x_3} (c_{f2}\Gamma - c_{f1}\delta_E) \, \mathrm{d}x, \qquad J_3(t) = \int_{x_0}^{x_3} c_{f1} \Gamma x \, \mathrm{d}x$$

$$J_4(t) = \int_{x_0}^{x_3} (c_{f2}\Gamma - c_{f1}\delta_E) x \, \mathrm{d}x$$

$$J_5(t) = \int_{x_0}^{x_3} c_D(\delta_E - \delta_c) \, \mathrm{d}x + [\delta_E(x_1) - \delta_c] c_{Dbp}$$

$$J_6(t) = \left(\frac{1}{L}\right) \int_{x_1}^{x_2} x \delta_E \rho_1 \, \mathrm{d}x$$

$$J_7 = -\left(\frac{i}{L}\right) \int_{x_1}^{x_2} [\rho_1 \dot{\delta}_E \bar{\delta}_E - \rho_2 a_d L(\dot{\Gamma} + 4i\dot{\phi}\Gamma + iq_2)\bar{\Gamma}] \, \mathrm{d}x$$

$$J_8(t) = a_d \int_{x_1}^{x_2} (\dot{\Gamma} - 2i\dot{\phi}\Gamma) \rho_2 \, \mathrm{d}x$$

Appendix B: Generalized Forces and Hermitian Polynomials

The forces and polynomials are

$$\mathrm{d}Q_{1x} = \frac{\mathrm{d}F_x}{\mathrm{d}x} \mathrm{d}x = -g_1 c_D(x) \, \mathrm{d}x$$

$$\mathrm{d}Q_{1y} + i \, \mathrm{d}Q_{1z} = \left[\frac{\mathrm{d}F_y}{\mathrm{d}x} + i\frac{\mathrm{d}F_z}{\mathrm{d}x} + (-\psi + i\theta)\frac{\mathrm{d}F_x}{\mathrm{d}x}\right] \mathrm{d}x$$

$$\mathrm{d}Q_{2x} = \frac{\mathrm{d}M_x}{\mathrm{d}x} \mathrm{d}x$$

$$\mathrm{d}Q_{2y} + i \, \mathrm{d}Q_{2z} = \left[x\left(\frac{\mathrm{d}F_y}{\mathrm{d}x} + i\frac{\mathrm{d}F_z}{\mathrm{d}x}\right) - \delta_E \frac{\mathrm{d}F_x}{\mathrm{d}x} - \theta \frac{\mathrm{d}M_x}{\mathrm{d}x}\right] \mathrm{d}x$$

$$Q_{1x} = F_x$$

$$Q_{1y} + i Q_{1z} = F_y + iF_z + (-\psi + i\theta) F_x$$

$$Q_{2x} = M_x$$

$$Q_{2y} + i Q_{2z} = -i(M_y + iM_z - iF_x\delta_c) - \theta M_x$$

$$N_1 = 1 - 3z^2 + 2z^3, \qquad N_1' = 6(z^2 - z)$$

$$N_2 = L_e z(1-z)^2, \qquad N_2' = L_e(1 - 4z + 3z^2)$$

$$N_3 = z^2(3 - 2z), \qquad N_3' = 6(z - z^2)$$

$$N_4 = L_e z^2(z - 1), \qquad N_4' = L_e(3z^2 - 2z)$$

Appendix C: Differential Equation Coefficients

For Eq. (45), where $m = 1, 2$,

$$R_{1n} = (md^2/L) a_{1n}, \qquad R_{2n} = (md^2/L)(a_{2n} + (a_d L) b_{2n} + x_c a_{1n})$$

$$S_{11} = (md)V + \left(g_1 d^2/V\right) c_2, \qquad S_{12} = x_c m d^2$$

$$S_{1n} = -\left(g_1 d^2/V\right)(g_{1n} + g_{a1n}), \qquad S_{21} = \left(g_1 d^2 V\right)(c_4 - x_c c_2)$$

$$S_{22} = I_{t0} + md^2 x_c^2, \qquad S_{2n} = -\left(g_1 d^2/V\right)(g_{2n} + g_{a2n}) - x_c S_{1n}$$

$$T_{11} = (g_1 d)(c_1 - C_D), \qquad T_{12} = (md)V$$

$$T_{1n} = -(g_1 d)(f_{1n} + f_{a1n}), \qquad T_{21} = (g_1 d)(c_3 - x_c c_1)$$

$$T_{2n} = -(g_1 d)\left(f_{2n} + f_{a2n} - C_D a_{1n} L^{-1} + h_{an}\right) - x_c T_{1n}$$

$$S_{2n}^* = -2(md^2) a_d b_{2n}, \qquad T_{22}^* = -I_x$$

$$t_{1D} = (\dot{\phi}^2 - i\ddot{\phi})\delta_{cB}, \qquad t_{2D} = (\dot{\phi}^2 - i\ddot{\phi})(J_{6B} + J_{8B1})$$

$$t_{1A} = J_{1B} + i(\dot{\phi} d/V) J_{2B}, \qquad t_{2A} = J_{3B} + i(\dot{\phi} d/V) J_{4B}$$

For Eq. (45) where $m > 2$,

$$R_{mn} = (md^2/L) k_{mn}$$

$$S_{m1} = (md)V a_{1m} L^{-1} - \left(g_1 d^2/V\right)(g_{m1} + g_{am1}), \qquad S_{m2} = R_{2m}$$

$$S_{mn} = -\left(g_1 d^2/V\right)(g_{mn} + g_{amn}) + (md^2/L)\left(2\omega_0^2/\omega_1\right)\hat{k} c_{mn}$$

$$T_{m1} = -(g_1 d)\left(f_{m1} + f_{am1} + C_D a_{1m} L^{-1}\right), \qquad T_{m2} = mdV a_{1m} L^{-1}$$

$$T_{mn} = -(g_1 d)(f_{mn} + f_{amn}) + (md^2/L)\omega_0^2 c_{mn} + 2\dot{\phi}^2 m d^2 a_d b_{mn}$$

$$S_{mn}^* = -4(md^2) a_d b_{mn}, \qquad T_{m2}^* = 2md^2 a_d b_{2m}$$

$$T_{mn}^* = -(md^2/L)\left(2\omega_0^2/\omega_1\right)\hat{k} c_{mn}$$

$$t_{mD} = (\dot{\phi}^2 - i\ddot{\phi})(k_{Bm}/L + 2a_d b_{Bm}) - 4i\dot{\phi}^2 a_d b_{Bm}$$

$$t_{3A} = f_{B3} + f_{aB3} + i(\dot{\phi} d/V)(g_{B3} + g_{aB3})$$

$$t_{4A} = f_{B4} + f_{a4B} + i(\dot{\phi} d/V)(g_{B4} + g_{a4B})$$

$$t_{mA} = f_{Bm} + i(\dot{\phi} d/V) g_{Bm} \qquad 4 < m < n_t - 1$$

$$t_{(n_t-1)A} = f_{B(n_t-1)} + f_{aB(n_t-1)} + i(\dot{\phi} d/V)\left(g_{B(n_t-1)} + g_{aB(n_t-1)}\right)$$

$$t_{n_t A} = f_{Bn_t} + f_{aBn_t} + i(\dot{\phi} d/V)\left(g_{Bn_t} + g_{aBn_t}\right)$$

Appendix D: Finned Missile Parameters

The parameters are as follows:

$$\rho_1 = \rho_2 = \rho_3 = 1, \qquad x_c = 0$$

$$L = 20, \qquad V = 6000 \text{ ft/s}$$

$$d = 0.35 \text{ ft}, \qquad \rho = 0.002 \text{ slug/ft}^3$$

$$m = 3.50 \text{ slug}, \qquad x_{01} = x_{23} = 1$$

$$I_x = 0.054 \text{ slug} \cdot \text{ft}^2, \qquad a_s = 1100 \text{ ft/s}$$

$$I_{t0} = 14.318 \text{ slug} \cdot \text{ft}^2, \qquad a_L = 2\left[\sqrt{(V/a_s)^2 - 1}\right]^{-1}$$

$$c_{f1} \begin{cases} = 4(11 - x), & 10 < x \le 11 \\ = e^{2(x-10)}, & -5 < x \le 10 \\ = -(2/\pi)(15 + 3x) a_L, & -7 < x \le -5 \\ = (12/\pi) a_L, & -11 \le x \le -7 \end{cases}$$

$$c_{f2}\begin{cases} = 2(11-x)^2, & 10 < x \le 11 \\ = 2 + 0.5\left(1 - e^{2(x-10)}\right), & -5 < x \le 10 \\ = 2.5 + (1/3\pi)(15+3x)^2 a_L, & -7 < x \le -5 \\ = 2.5 - (12/\pi)(6+x)a_L, & -11 \le x \le -7 \end{cases}$$

$$c_D\begin{cases} = (0.30)(11-x), & 10 < x \le 11 \\ = 0, & x \le 10 \end{cases}$$

$$C_{Dbp} = 0.14, \qquad C_{\ell p} = -18$$

$$d_{11} = 0, \qquad d_{21} = 0$$

$$d_{12} = 10^{-3}, \qquad d_{22} = -0.25 \times 10^{-5}$$

$$C_{N\alpha} = 9.7, \qquad C_{M\alpha} = -34.4$$

$$C_{Mq} = -980, \qquad C_{M\dot{\alpha}} = -190$$

References

[1]Mikhail, A. G., "In-Flight Flexure and Spin Lock-in for Antitank Kinetic Energy Projectiles," *Journal of Spacecraft and Rockets*, Vol. 33, No. 5, 1996, pp. 657–664.

[2]Guidos, B. J., Garner, J. M., Newill, J. F., and Livecchia, C. D., "Measured In-Flight Rod Flexure of a 120mm M829E3 Kinetic Energy (KE) Projectile Steel Model," U.S. Army Research Lab., ARL-TR-2820, Aberdeen Proving Ground, MD, Sept. 2002.

[3]Peppitone, T. R., and Jacobson, J. D., "Resonant Behavior of a Symmetric Missile Having Roll Orientation: Dependent Aerodynamics,"*Journal of Guidance and Control*, Vol. 1, No. 5, 1978, pp. 335–339.

[4]Grover, L. S., "Effects on Roll Rate of Mass and Aerodynamic Asymmetries on Ballistic Re-Entry Bodies," *Journal of Spacecraft and Rockets*, Vol. 2, No. 2, 1965, pp. 220–225.

[5]Price, D. A., Jr., "Sources, Mechanisms and Control of Roll Resonance Phenomena for Sounding Rockets," *Journal of Spacecraft and Rockets*, Vol. 4, No. 11, 1967, pp. 1516–1525.

[6]Price, D. A., Jr., and Ericsson, L. E., "A New Treatment of Roll–Pitch Coupling for Ballistic Re-Entry Bodies," *AIAA Journal*, Vol. 8, No. 9, 1970, pp. 1608–1615.

[7]Murphy, C. H., "Some Special Cases of Spin–Yaw Lock-In," *Journal of Guidance, Control, and Dynamics*, Vol. 12, No. 6, 1989, pp. 771–776.

[8]Platus, D. H., "Aeroelastic Stability of Slender, Spinning Missiles," *Journal of Guidance, Control, and Dynamics*, Vol. 15, No. 1, 1992, pp. 144–151.

[9]Legner, H. H., Lo, E. Y., and Reinecke, W. G., "On the Trajectory of Hypersonic Projectiles Undergoing Geometry Changes," AIAA Paper 94-0719, Jan. 1994.

[10]Heddadj, S., Cayzac, R., and Renard, J., "Aeroelasticity of High L/D Supersonic Bodies: Theoretical and Numerical Approach," AIAA Paper 2000-0390, Jan. 2000.

[11]Murphy, C. H., and Mermagen, W. H., "Flight Mechanics of an Elastic Symmetric Projectile," *Journal of Guidance, Control, and Dynamics*, Vol. 24, No. 6, 2001, pp. 1125–1132.

[12]Murphy, C. H., and Mermagen, W. H., "Flight Motion of a Continuously Elastic Finned Missile," *Journal of Guidance, Control, and Dynamics*, Vol. 26, No. 1, 2003, pp. 89–98.

[13]Murphy, C. H., and Mermagen, W. H., "Flight Motion of a Continuously Elastic Finned Missile," U.S. Army Research Lab., ARL TR-2754, AD A405876, Aberdeen Proving Ground, MD, June 2002.

[14]Geradin, M., and Rixen, D., *Mechanical Vibrations: Theory and Applications to Structural Dynamics*, Wiley, Chichester, England, U.K., 1994, pp. 263–293.

[15]Murphy, C. H., "Free Flight Motion of Symmetric Missiles," U.S. Army Research Lab., BRL Rept. 1216, AD 442757, Aberdeen Proving Ground, MD, July 1963.

[16]Murphy, C. H., and Mermagen, W. H., "Spin–Yaw Lockin for an Elastic Finned Projectile," U.S. Army Research Lab., Rept. TR 3217, Aberdeen Proving Ground, MD, June 2004.

[17]deSilver, C. W., *Vibration Fundamentals and Practice*, CRC Press, New York, 2000, p. 351.

[18]Dorman, J. R., and Prince, P. J., "A Family of Embedded Runge–Kutta Formulae," *Journal of Computational and Applied Mathematics*, Vol. 6, 1980, pp. 18–26.